

Observations of Ice Crystal Habits with a Scanning Polarimetric W-Band Radar at Slant Linear Depolarization Ratio Mode

SERGEY Y. MATROSOV

Cooperative Institute for Research in Environmental Sciences, University of Colorado, and NOAA/Earth System Research Laboratory, Boulder, Colorado

GERALD G. MACE

Department of Atmospheric Sciences, University of Utah, Salt Lake City, Utah

ROGER MARCHAND

Joint Institute for Study of Atmosphere and Ocean, University of Washington, Seattle, Washington

MATTHEW D. SHUPE

Cooperative Institute for Research in Environmental Sciences, University of Colorado, and NOAA/Earth System Research Laboratory, Boulder, Colorado

ANNA G. HALLAR AND IAN B. MCCUBBIN

Division of Atmospheric Sciences, Desert Research Institute, Reno, Nevada, and Storm Peak Laboratory, Steamboat Springs, Colorado

(Manuscript received 3 August 2011, in final form 19 March 2012)

ABSTRACT

Scanning polarimetric W-band radar data were evaluated for the purpose of identifying predominant ice hydrometeor habits. Radar and accompanying cloud microphysical measurements were conducted during the Storm Peak Laboratory Cloud Property Validation Experiment held in Steamboat Springs, Colorado, during the winter season of 2010/11. The observed ice hydrometeor habits ranged from pristine and rimed dendrites/stellars to aggregates, irregulars, graupel, columns, plates, and particle mixtures. The slant 45° linear depolarization ratio (SLDR) trends as a function of the radar elevation angle are indicative of the predominant hydrometeor habit/shape. For planar particles, SLDR values increase from values close to the radar polarization cross coupling of about -21.8 dB at zenith viewing to maximum values at slant viewing. These maximum values depend on predominant aspect ratio and bulk density of hydrometeors and also show some sensitivity to particle characteristic size. The highest observed SLDRs were around -8 dB for pristine dendrites. Unlike planar-type hydrometeors, columnar-type particles did not exhibit pronounced depolarization trends as a function of viewing direction. A difference in measured SLDR values between zenith and slant viewing can be used to infer predominant aspect ratios of planar hydrometeors if an assumption about their bulk density is made. For columnar hydrometeors, SLDR offsets from the cross-coupling value are indicative of aspect ratios. Experimental data were analyzed for a number of events with prevalence of planar-type hydrometeors and also for observations when columnar particles were the dominant species. A relatively simple spheroidal model and accompanying T-matrix calculations were able to approximate most radar depolarization changes with viewing angle observed for different hydrometeor types.

Corresponding author address: Sergey Y. Matrosov, R/PSD2,
325 Broadway, Boulder, CO 80305.
E-mail: sergey.matrosov@noaa.gov

1. Introduction

Ice hydrometeor type and habit (shape) information is essential for modeling cloud life cycles (e.g., Avramov

and Harrington 2010) because particle habit influences crucial processes, including crystal growth, evaporation rate, ice crystal fall speed, and cloud radiative properties. Characterization of ice hydrometeor habits is recognized by the U.S. Department of Energy's (DoE's) Atmospheric System Research (ASR) Program as one of the important research objectives for improving atmospheric models at different scales. Precipitation formation processes are also significantly affected by ice hydrometeor habits, which to a certain degree determine the efficiency of collision and coalescence. Ice particle habit and orientation information is also important in many active and passive remote sensing applications at different spectral regions because scattering phase functions and backscatter properties of ice clouds and snowfall exhibit significant dependence on particle types and alignment (e.g., Liu 2008).

Precipitation polarimetric radars are operated at longer wavelengths λ [e.g., at S band ($\lambda \sim 10$ cm), C band ($\lambda \sim 5$ cm), or X band ($\lambda \sim 3$ cm)]. Such radars have been used for hydrometeor identification using reflectivity data and polarimetric measurements of differential reflectivity Z_{DR} , the copolar correlation coefficient ρ_{hv} , and, sometimes, specific differential phase shift K_{DP} (e.g., Ryzhkov et al. 2005). These measurements can generally discriminate between regions of pristine ice crystals and highly aggregated snow crystals. However, particle-type recognition such as distinguishing among planar ice crystals (e.g., dendrites and plates) and columnar ice crystals (e.g., bullets, columns, and needles) and inferring particle aspect ratios is generally problematic from traditional polarimetric measurements.

Cloud radars usually operate at higher frequencies, such as those at K_a band ($\lambda \sim 0.8$ cm) and W band ($\lambda \sim 0.3$ cm; e.g., Kollias et al. 2007). These radars are used for shorter ranges, compared to precipitation radars, and typically provide higher spatial resolution. The polarimetric cloud radars generally implement technology, consisting in the reception of copolar and cross-polar returns. This provides a measurement of depolarization ratio (DR), which for the case of linear polarization transmission is defined as the logarithmic difference between measured cross-polarized (Z_{cr}) and copolarized (Z_{co}) equivalent reflectivity factors (hereafter just reflectivities) in the linear scale ($\text{mm}^6 \text{m}^{-3}$),

$$\text{DR}(\text{dB}) = 10 \log_{10}(Z_{cr}) - 10 \log_{10}(Z_{co}). \quad (1)$$

Many cloud radars, including most new DoE Atmospheric Radiation Measurement (ARM) Program cloud radars, transmit horizontally polarized signals and receive horizontally (H) and vertically (V) polarized returns, thus providing measurements of H–V linear

depolarization ratio (LDR). Some other cloud radars [e.g., the ARM millimeter wave cloud radar (MMCR)] transmit circular polarization signals and, in this case, measurements of co- and cross-polarized returns provide CDR. Other types of DR include slant linear depolarization ratio (SLDR), which is measured when an H–V system is tilted at some angle (e.g., by 45°).

Some earlier studies with the K_a -band DR measurements (Matrosov et al. 2001; Reinking et al. 2002) indicated the usefulness of CDR and 45° SLDR data for ice particle type and shape estimations. The renewed interest in the ice particle habit estimation from polarimetric cloud radar measurements is determined, in part, by the importance of habit information for model studies and by the fact that scanning polarimetric cloud radars are becoming more widely available for the atmospheric science community.

All stations within the ARM Climate Research Facility (ACRF) are currently being equipped with scanning polarimetric cloud radars. The first of such radars, namely, the scanning W-band cloud radar (SWACR), was recently deployed as part of the Storm Peak Laboratory Cloud Property Validation Experiment (StormVEx) held in Steamboat Springs, Colorado, during the November 2010–April 2011 period. One of the main objectives of the StormVEx field deployment was collecting correlative datasets for validating multisensor cloud parameter retrievals. These datasets included measurements from a multitude of remote sensors deployed at the valley floor at an altitude of about 2060 m above mean sea level (MSL) and at the midslope of the Storm Peak (~ 2760 m MSL), where the SWACR was located. In situ cloud data were collected at the Desert Research Institute's Storm Peak Laboratory (SPL) located at a distance of 2.4 km and 0.44 km above the SWACR.

The objective of this study is to evaluate capabilities of scanning W-band radar polarimetric measurements for the purpose of inferring ice hydrometeor habits by comparing measured depolarization ratio patterns and particles observed at the SPL. The W band is the highest frequency band used in operational ground-based cloud radars and many hydrometeors are already outside the Rayleigh scattering regime for this frequency band. This makes depolarization modeling more complicated and observed depolarization patterns not as distinct as for lower cloud radar frequencies.

A number of computational techniques and particle models have been used for calculating radar copolarized backscatter and traditional polarimetric parameters (e.g., differential reflectivity, and linear horizontal–vertical depolarization ratio). Nonspherical particle models include simple oblate and prolate spheroids (e.g., Matrosov 1991, 2007; Hogan et al. 2012) and more complex shapes

(e.g., Schneider and Stephens 1995; Liu 2008; Ishimoto 2008; Petty and Huang 2010). The computational techniques range from the T-matrix method for spheroids, to the finite-difference time domain method (e.g., Aydin and Tang 1997), the discrete dipole approximation (e.g., Okamoto 2002), the Rayleigh Gans theory (e.g., Westbrook et al. 2006), and generalized multiparticle Mie methods (e.g., Grecu and Olson 2008). Reviews and comparisons of different models/methods studies can be found in Botta et al. (2011) and Kneifel et al. (2011). The slant linear depolarization ratio, however, has not been modeled in the studies mentioned above.

While this study is mostly concerned with analyzing measured SLDR and simultaneous observations of hydrometeor habits during StormVEx, some initial theoretical estimates of the radar observables are presented for illustration purposes. These estimates are based on the relatively simple spheroidal particle model and T-matrix calculations. Detailed comparisons of the SLDR calculations made using different ice hydrometeor models and computational methods deserve additional theoretical research and are outside the scope of this study.

It is instructive to assess SWACR's particle habit sensitivity since during StormVEx collocated radar and in situ particle observations were made with a frequency that is much higher than is typically achieved when only airborne sensors are used for in situ sampling. Because a number of scanning cloud polarimetric radars, including those operating at W band, are being deployed at many ACRF sites, testing new approaches for radar-based particle habit recognition is also beneficial for future studies.

2. SWACR polarimetric measurables and their calibration by observing spherical targets

The SWACR was manufactured by ProSensing, Inc. Originally a vertically pointing 95-GHz radar, it was upgraded for scanning in 2009. A range resolution of about 43 m was used during StormVEx. The antenna beamwidth of 0.3° provided an excellent cross-beam resolution. The radar scan rate of 4° s^{-1} and the pulse repetition frequency of 10 kHz were used in a scanning mode. The SWACR uses linear transmitted polarization with alternating reception of copolar and cross-polar echoes. A slant 45° linear polarization transmission was employed by the SWACR during StormVEx. This transmission type was chosen for this study because the resulting depolarization ratios depend relatively little on ice particle flutter around their preferential orientation with major dimensions in the horizontal plane, which is caused by aerodynamic forcing. As a result, SLDR changes are influenced mostly by particle shapes (habits). For the traditional horizontal and vertical polarization basis, the particle orientation

and shape effects are difficult (and in many instances impossible) to decouple. While rotating the linear polarization basis generally does not affect vertically pointing radar measurements, 45° SLDR is better suited than H-V LDR for particle shape estimation at slant viewing (Matrosov et al. 2001; Reinking et al. 2002). Although CDR generally exhibits less sensitivity to particle orientation than different linear depolarization ratios and is more preferable for estimating hydrometeor shapes (Matrosov et al. 1996), the circular polarization measurement scheme was not employed in StormVEx because of a more complicated implementation of this scheme with the SWACR.

SLDR, and other depolarization ratio types, do not depend on the radar absolute calibration, and it is not affected by attenuation of radar signals in liquid water and atmospheric gases because the attenuation rates in these substances are the same for both copolar and cross-polar radar returns. Bias in depolarization ratios resulting from differential propagation phase is usually small in ice clouds and for shorter ranges can be neglected (Matrosov et al. 2001).

The SWACR operated during StormVEx in a repeating 30-min scanning protocol. About 60% of each interval was reserved for pointing vertically. Full Doppler spectra measurements were recorded during this operational mode. During the remaining 40% of the time interval, two plan-position indicator (PPI) scans, fixed-beam SPL pointing measurements, and different azimuthal direction range–height indicator (RHI) scans were performed. Only Doppler spectra moment measurements were available during the scanning modes. One of the RHI scans was oriented toward the SPL, providing cross sections of radar measurements in a vertical plane containing the radar site and the SPL.

Radar hardware is always imperfect (e.g., Brunkow et al. 2000). Imperfections result in polarization “cross coupling” (e.g., resulting from antenna finite polarization isolation). As a result, depolarization ratio measurements are biased (e.g., Galletti et al. 2012) compared to intrinsic values that would be observed with perfect radar hardware. Decoupling depolarization measurements is complex and it is outside the scope of this study. Measured SLDR values are, however, still valuable and can be used to gain information on ice hydrometeor habits.

a. Observation of freezing drizzle

Estimating the magnitude of cross coupling is important for interpreting results of the SWACR depolarization measurements. Observations of small drizzle drops, which are spherical, provide an opportunity for such estimations. Freezing drizzle was observed at the SPL and the mountain slopes by the operators and StormVEx scientists at around 1800 UTC 16 January 2011. Figure 1 shows the SWACR RHI measurements

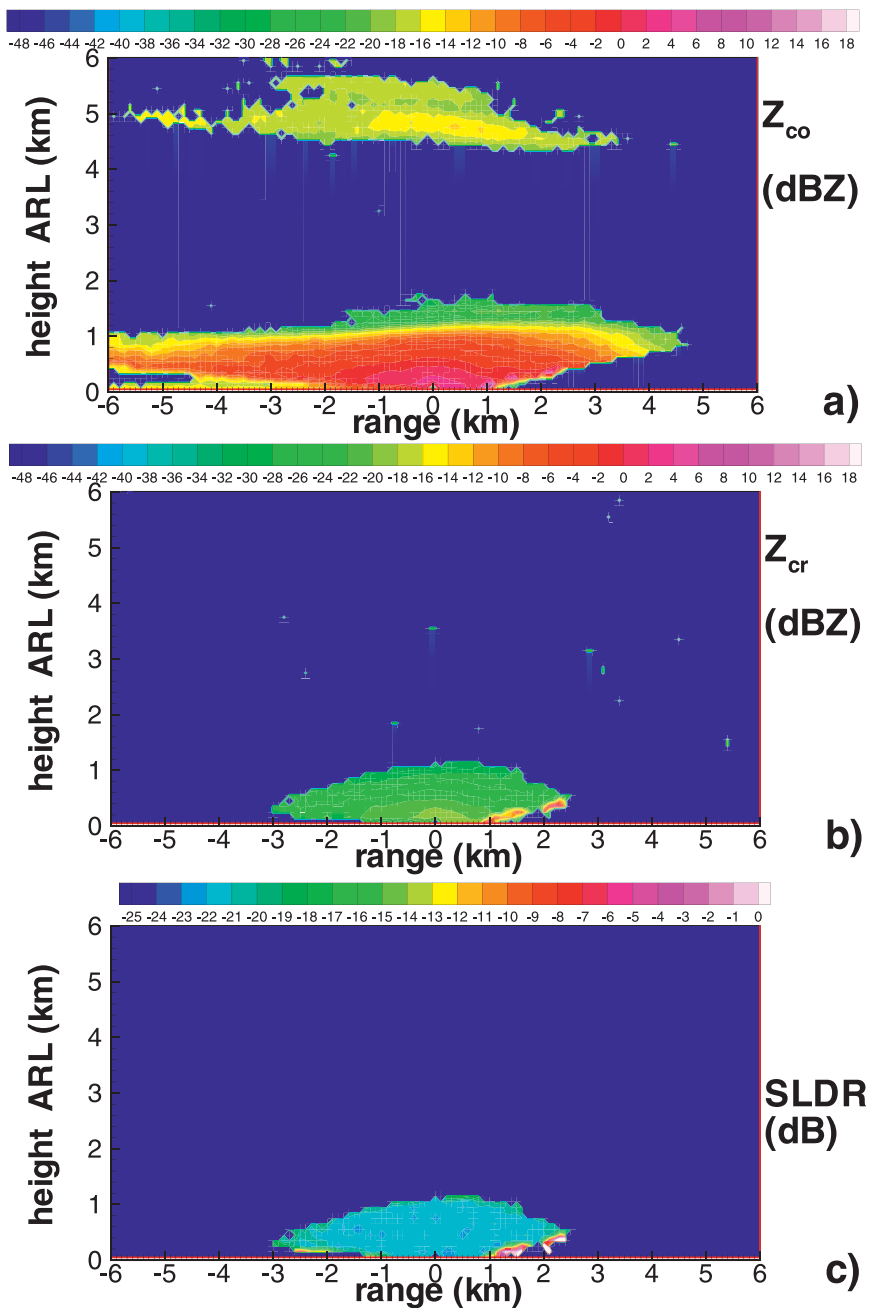


FIG. 1. SWACR measurements of (a) copolar and (b) cross-polar reflectivity and (c) SLDR during the RHI scan toward the SPL ($az = 87.1^\circ$) when observing freezing drizzle at 1800 UTC 16 Jan 2011.

toward the SPL (i.e., in the 87.1° azimuthal direction) at this particular time. The SPL is located at a distance of about 2.4 km and along the 11° elevation line to the right of the coordinate origin in this figure. The mountain slope blocks measurements for lower elevations in this direction (corresponding ground clutter can be seen in Fig.1 beyond the range of 1 km at the lowest elevation angles). The area of the copolar returns in Fig. 1 is larger

compared to the area of cross-polar returns because Z_{cr} is significantly weaker than Z_{co} , and at longer distances from the radar Z_{cr} values (and thus SLDR values) are near the noise level. The upper cloud observed at a height of about 5 km above the radar level (ARL) in the copolar radar channel is not seen in the cross-polar channel. SLDR values in Fig. 1c are generally between -21 and -22 dB except at the echo fringes, which is

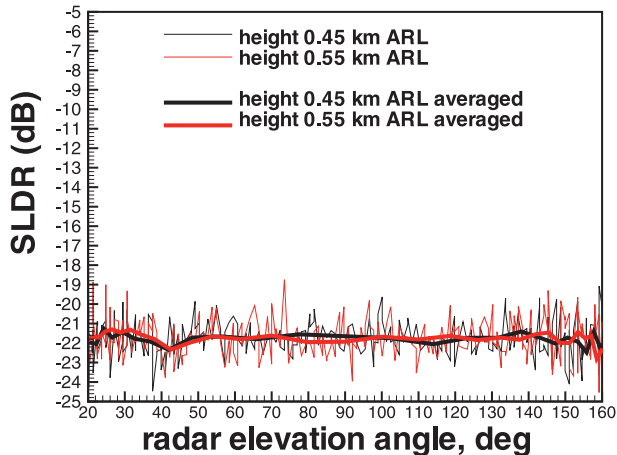


FIG. 2. Instantaneous and averaged measurements of SLDR at 0.45 and 0.55 km ARL during the RHI scan toward the SPL ($az = 87.1^\circ$) when observing freezing drizzle at 1800 UTC 16 Jan 2011.

caused by low Z_{cr} signal-to-noise ratios, and the ground clutter caused by the mountain slope. Preliminary estimates of liquid water path (LWP) using statistical retrievals from a two-channel (23.8 and 31.4 GHz) vertically pointing microwave radiometer (MWR), which was collocated with the SWACR, were between 200 and 300 $g\ m^{-2}$ at the time of the RHI scan depicted in Fig. 1. Details on the ARM MWR retrievals and calibrations can be found online (<http://www.arm.gov/instruments/mwr>).

Figure 2 shows the elevation angle SLDR dependences at constant altitudes of 0.45 and 0.55 km ARL. Individual SLDR measurements are somewhat noisy. Typical standard deviations are about 0.8–1 dB, which is not unusual given the nature of fluctuating targets. The averaged (in $0.15\ km \times 0.15\ km$ cells) SLDR estimates are also shown in Fig. 2. As expected, there is no elevation angle dependence of SLDR for spherical drizzle drops. The mean value of SLDR is $-21.8\ dB$, which is independent of altitude.

For the ideal hardware there is no cross-polar return for spherical targets. The $-21.8\ dB$ minimum measurable SLDR value is determined by the polarization cross coupling for the StormVEx SWACR slant 45° linear polarization measurements. The degradation of cross-polar isolation from the SWACR value of about $-27\ dB$ for the standard horizontal–vertical polarization basis might be due to some unknown factors influencing radar hardware when rotating the linear polarization basis. However, as will be shown below, this relatively poor cross-polar isolation does not preclude the SWACR from performing valuable depolarization measurements (though biased) that are indicative of ice hydrometeor habits.

b. Observations of rounded graupel

On 14 January 2011 rounded graupel was observed at the SPL and nearby slopes after about 2100 UTC. Characteristic SWACR RHI measurements in the direction of the SPL (i.e., 87.1°) are shown in Fig. 3. As for the case with freezing drizzle, the cross-polar signals from the upper cloud parts and at longer ranges were in the noise, and SLDR values could only be estimated at the closer ranges for the lower precipitating cloud containing rounded quasi-spherical graupel. The upper frame of Fig. 4 shows a sample photograph of observed particles. The particle effective diameters were about 0.4–0.5 mm as inferred from the Droplet Measurement Technologies (DMT) precipitation imaging probe (PIP), which was modified for ground-based use and operated at the SPL. The MWR-based preliminary estimates of LWP were around 200–300 $g\ m^{-2}$, and the DMT signal processing package (SPP)-100 for the forward scattering spectrometer probe (FSSP) at the SPL was estimating cloud liquid water content (LWC) generally around 0.1 $g\ m^{-3}$ around the depicted RHI scan time. Note that while radar echoes are dominated by larger ice particles, supercooled liquid water influences riming and is thus an important factor influencing the shape of ice hydrometeors. The detailed descriptions of DMT probes are available online (<http://www.dropletmeasurement.com>).

Constant-altitude (0.45 km) SLDR instantaneous and averaged (in $0.15\ km \times 0.15\ km$ cells) measurements corresponding to a scan in Fig. 3 are shown in Fig. 4. The mean SLDR value is about $-21.4\ dB$, which is only marginally higher than that for the case of spherical drizzle drops (i.e., $-21.8\ dB$), but still measurable if averaging with respect to the viewing angle is performed. The small mean SLDR difference (i.e., 0.4 dB) can possibly be explained by imperfect roundness and possible tumbling of the observed graupel particles. Similar (~ 0.4 – $0.5\ dB$) differences in depolarization ratios of drizzle and graupel were observed with the National Oceanic and Atmospheric Administration (NOAA) K_a -band radar (Reinking et al. 1997).

3. Observations of pristine and rimed dendrites

Events with precipitating clouds were common during StormVEx. Dendritic crystal habits with different degrees of riming were observed at the SPL during these events. Riming changes particle aspect ratios. It was previously found that a spheroidal model adequately describes traditional (e.g., Hogan et al. 2012; Schneider and Stephens 1995) and depolarization (Matrosov et al. 2001) radar properties of different ice hydrometeors.

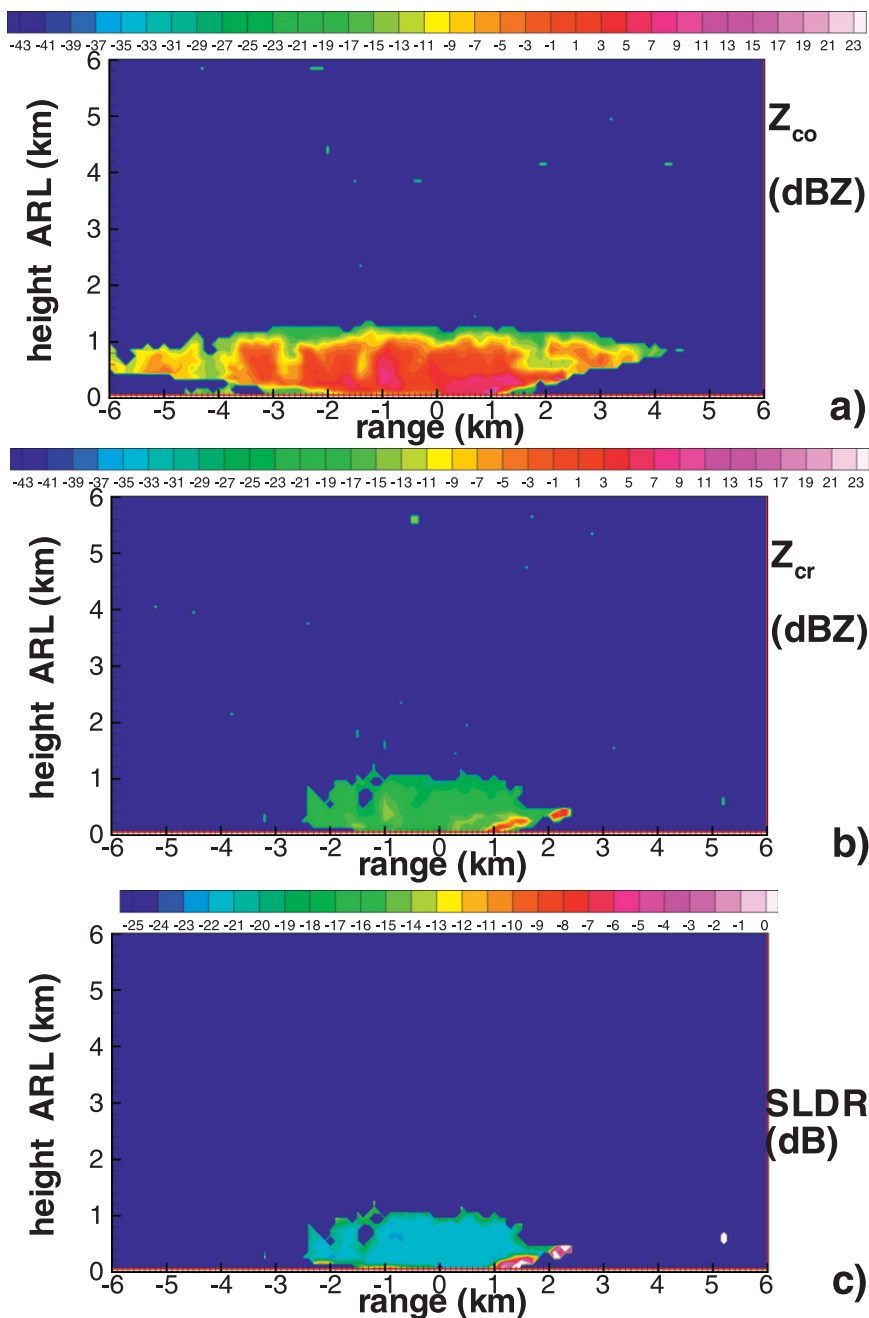


FIG. 3. SWACR measurements of (a) copolar and (b) cross-polar reflectivity and (c) SLDR during the RHI scan toward the SPL ($az = 87.1^\circ$) when observing round graupel at 2228 UTC 14 Jan 2011.

Pristine dendritic crystals and their varieties (e.g., stellars) are modeled here as oblate spheroids. Such crystals have typical aspect ratios r of about 0.04–0.12 and effective densities ρ of about 0.4–0.7 g cm^{-3} (Pruppacher and Klett 1978). The oblate model with these parameters was found to be in good agreement with K_a -band radar measurements of dendritic crystals (Reinking et al.

2002), so an attempt was made here to apply the spheroidal particle model for W band too. As a result of rimming, particles become more spherical and their aspect ratios increase. Graupel particles are an extreme example of rimming. Because SLDR values strongly depend on particle shape, it is instructive to analyze SWACR measurements of dendritic crystals with different degrees of rimming.

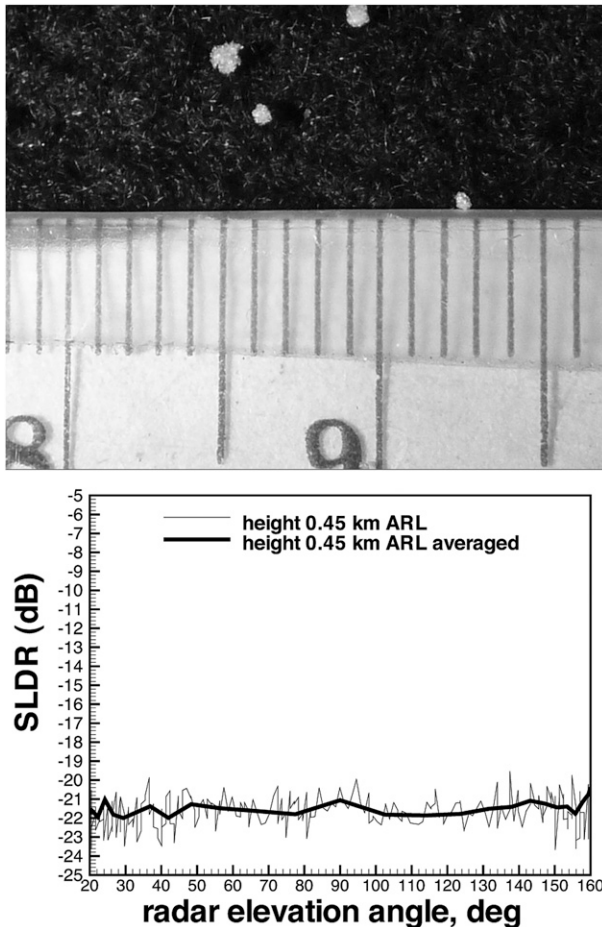


FIG. 4. (top) A particle photograph (small ruler ticks are millimeters) and (bottom) the instantaneous and averaged measurements of SLDR at 0.45 km ARL during the RHI scan toward the SPL ($az = 87.1^\circ$) when observing round graupel (for corresponding RHI scans see Fig. 3).

a. Observations of pristine dendritic crystals

Figure 5 shows an SWACR RHI at the 87.1° azimuth during a typical event when pristine dendritic crystals were observed at the SPL. The MWR-based estimates of LWP during such events effectively showed no measurable liquid water, and typical averaged PIP measurements of the particle effective diameter were around 1–1.5 mm, although individual crystals could be as large as 3 mm. A photograph of crystals sampled at around the time of the depicted RHI scan at 1700 UTC 11 February 2011 is shown in the upper frame of Fig. 6. Wind speeds measured near the SPL at the time of observations were at around 6 m s^{-1} .

Unlike for the drizzle and rounded graupel cases, the SLDR (Fig. 5c) of dendrites exhibits a very strong depolarization dependence on the radar elevation angle, reflecting a high degree of preferential horizontal orientation of particles. Note that if the particle orientation

were random, then the SLDR would not exhibit any trends with the radar elevation angle because such particle populations would look the same from all viewing directions. The observed SLDR values in Fig. 6 are relatively symmetrical with respect to the zenith direction.

The constant-altitude elevation angle dependencies of measured SLDR are shown in Fig. 6 (middle frame) for different heights above the radar site. There is not much variability in the SLDR measurements with height, suggesting that habits may not be changing significantly with altitude. The mean SLDR at vertical viewing is around the radar hardware polarization cross-coupling limit of -21.8 dB , which is explained by the quasi-spherical projections of preferably horizontally oriented dendrites. Very high depolarization of about -8 to -10 dB is seen at low viewing angles.

Figure 6 also depicts theoretical calculations of depolarization ratios for a model of oblate spheroids assuming different aspect ratios r and bulk densities ρ . The theoretical estimates are shown here for illustrative purposes, and they approximately account for the -21.8-dB cross-coupling effects. The use of more sophisticated particle models, computational approaches, and exact corrections for cross coupling also needs to be explored in the context of observed radar polarimetric parameters. This is, however, left for future research, because the purpose of this study is primarily to present observational evidence of SLDR sensitivity to ice hydrometeor types/habits.

For modeling estimates here it was assumed that the mean orientation of dendrites is horizontal (which is supported by the general symmetry of the RHI measurement patterns) and the standard deviation (SD) around this mean orientation is 9° . This estimate of standard deviation is based on earlier measurements with the NOAA scanning K_a -band polarimetric cloud radar when SLDR and traditional (i.e., when using horizontal and vertical polarization states) LDR were used to infer this quantity independently (Matrosov et al. 2005b). While SLDR measurements are not very sensitive to the standard deviation of the orientation (as long as it is relatively small), LDR data strongly depend on the standard deviation. When both SLDR and LDR are available simultaneously, shape and orientation effects can be decoupled and SD estimates can be obtained (Matrosov et al. 2005b) for situations when one single planar hydrometeor habit dominates radar returns. Changing the assumption about the orientation standard deviation between 0° and 15° does not significantly affect the SLDR modeling results (Matrosov et al. 2001). The corresponding SLDR variations are generally within 1 dB, which is on the order of the depolarization ratio noise for individual measurements. The T-matrix approach (Barber and Yeh 1975) was used for calculations.

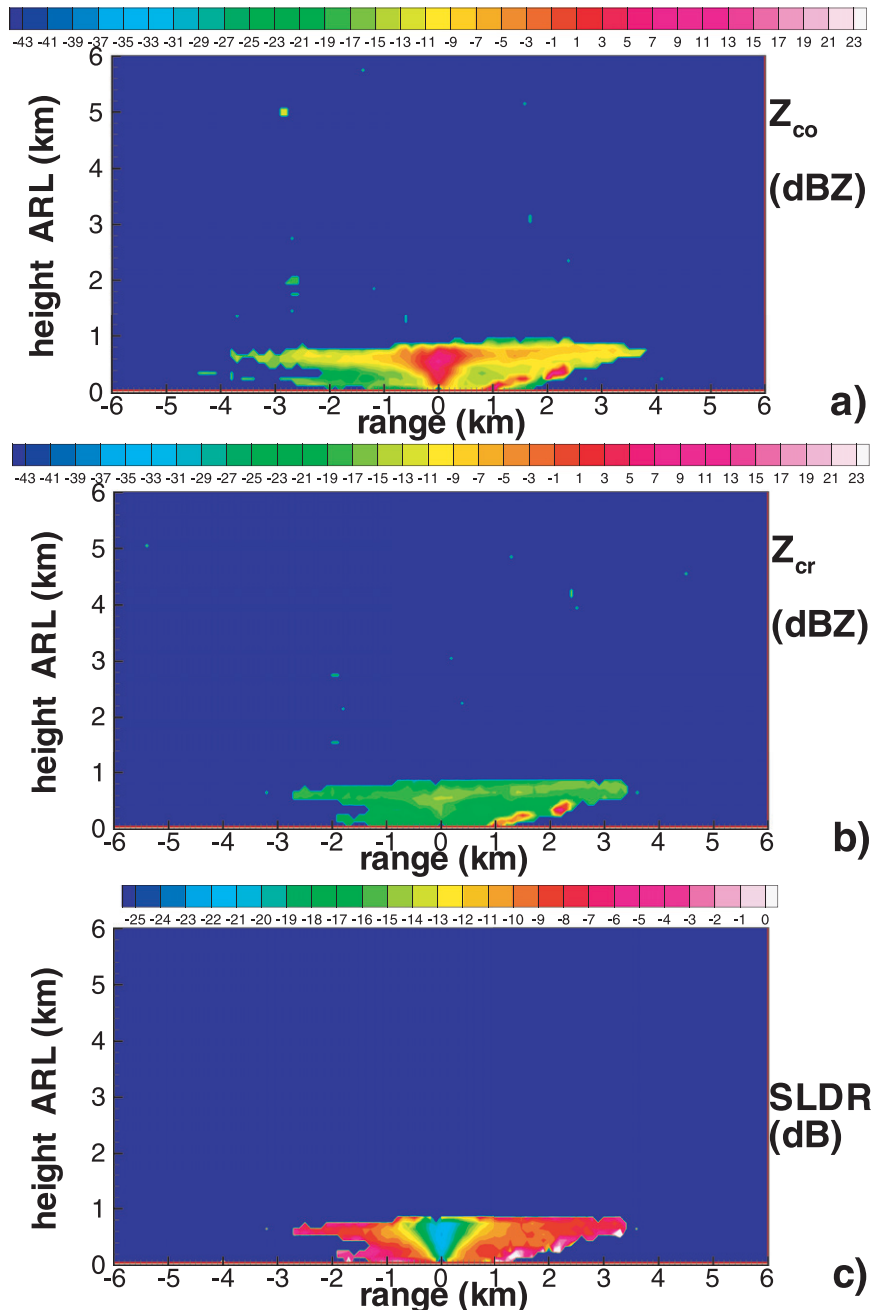


FIG. 5. SWACR measurements of (a) copolar and (b) cross-polar reflectivity and (c) SLDR during the RHI scan toward the SPL ($az = 87.1^\circ$) when observing pristine dendrites at 1700 UTC 11 Feb 2011.

In Fig. 6 (middle frame) a relatively simple oblate spheroidal model describes the SWACR SLDR data fairly well for the aspect ratio and bulk density of 0.11 and 0.65 g cm^{-3} , respectively. For low radar elevation angles, model estimates of SLDR for this assumption set are somewhat lower than those observed (particularly at slant elevations), suggesting that the assumed value of aspect ratio may be a little too large for single pristine

crystals. The T-matrix method, however, becomes increasingly unstable when calculating scattering properties of particles with very small aspect ratios, and the value of 0.11 was the smallest possible for calculations using this method for this example. This limitation precluded theoretical estimates for smaller aspect ratios, which could be more suitable for single pristine dendrites.

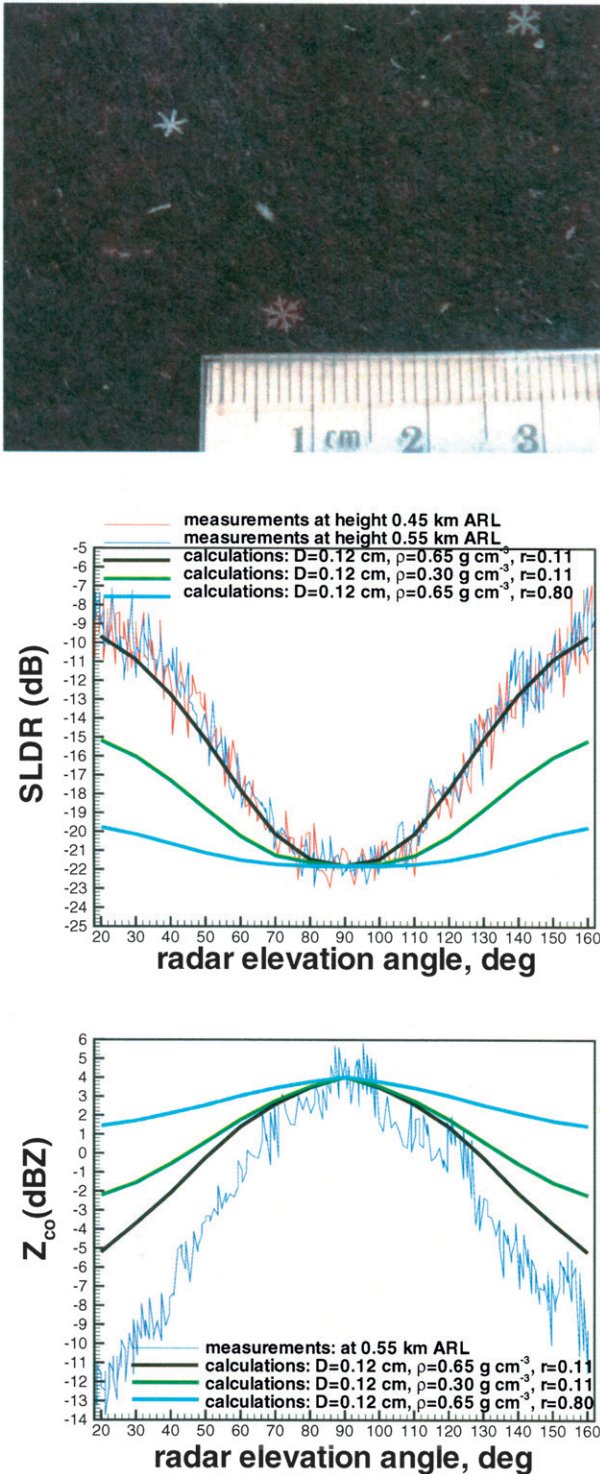


FIG. 6. (top) A particle photograph, (middle) SLDR, and (bottom) Z_{co} measurements and calculations for the RHI scan shown in Fig. 5.

There are no significant changes in observed SLDR measurements with height (thin red and blue curves in the middle frame of Fig. 6) suggesting that particle habits were not varying with altitude very much. A modest variability in particle characteristic size D (e.g., the median volume size) does not result in significant changes of SLDR values for the considered size range. For the same bulk density, an increase in aspect ratio (resulting in more spherical particles) causes a decrease in SLDR. The same shape particles exhibit higher depolarization when the bulk density is greater. To show the effects of changes in r and ρ , calculations for less dense ($\rho = 0.7 \text{ g cm}^{-3}$) and more spherical ($r = 0.8$) particles are also shown in Fig. 6.

One feature seen in pristine dendrite RHI measurements (Fig. 5) is an enhancement in absolute reflectivity Z_{co} near the zenith direction. Figure 6 (lower frame) shows elevation angle dependence of copolar reflectivity at a constant height of 0.55 km ARL. This enhancement is the combined results of non-Rayleigh scattering effects and particle orientation, shape, and density. The T-matrix calculations for different assumptions of aspect ratios, densities, and effective diameters of snowflakes are also shown. These calculations were scaled to match mean observed reflectivities in the zenith direction (no scaling is necessary for SLDR because it does not depend on particle concentration). Because the elevation angle trends of Z_{co} are of interest here, the exact absolute calibration of the SWACR is not important (note that the absolute calibration of the SWACR is still an ongoing activity). The modeling results indicate that the degree of the zenith angle reflectivity enhancement increases as particle density increase. The enhancement also increases as particle aspect ratios decrease (for a given density value). A somewhat similar effect of W-band reflectivity enhancement related to particle nonsphericity was observed with nadir-pointing W-band airborne radar (Matrosov et al. 2005a).

The set of assumptions about particle properties, which somewhat underestimates the SLDR magnitude at low elevation angles (i.e., the black curves in Fig. 6), also underestimates the decrease of the main (copolar) channel reflectivity when the viewing direction moves off zenith. Because calculations show that for slant viewing there is a general tendency for SLDR to increase and Z_{co} to decrease as the aspect ratio r gets smaller (given that the other assumptions are the same), this also may suggest that an assumption of $r < 0.1$ might better describe the observed results of Z_{co} elevation angle trends. The T-matrix method version utilized here, however, could not be used for such small values of r .

Particle size changes can cause greater variability in the degree of copolar reflectivity enhancement compared to the variability in SLDR. This fact can be explained, in part, by non-Rayleigh scattering effects, which are similarly manifested in larger particle backscatter cross sections on both polarizations. These effects are somewhat muted in the ratio of integrated backscatter cross sections (i.e., in SLDR). Modeling results also suggest (not shown) that compared to the slant 45° polarization, the rate of the reflectivity fall off from the maximum values in the zenith direction is smaller if the horizontal polarization is transmitted.

b. Observations of rimed dendritic crystals

Slightly rimed dendrites were the predominant ice hydrometeors during the periods of the event observed on 26 January 2011. The SWACR RHI in the azimuthal direction of 87.1° performed at 1823 UTC is shown in Fig. 7, and the particle photograph taken at the SPL is depicted in the upper frame of Fig. 8. The precipitating cloud depth was between 0.8 and 1 km, which is similar to the pristine dendrite case analyzed in the previous subsection. Preliminary MWR-derived estimates of LWP during at this time were around 100 g m^{-2} , and FSSP LWC estimates were generally under 0.03 g cm^{-3} . The SPL wind speeds were around $1\text{--}2 \text{ m s}^{-1}$, and the PIP-derived mean effective diameters were around 0.05–0.1 cm.

Figure 8 shows the constant-altitude elevation angle SLDR and copolar reflectivity dependences for the RHI scan shown in Fig. 7. As for the case of pristine dendrites, there are no significant differences in SLDR elevation angle patterns at different RHI azimuths (not shown). The theoretical curves shown by black lines in Fig. 8 are for the same of assumptions that were made for modeling results depicted by black lines in Fig. 6. In the lower frame of Fig. 8, the theoretical curve was scaled to the observational values at the zenith direction. Overall, there is a fair agreement for the base theoretical assumptions for both SLDR and Z_{co} in Fig. 8. Because slightly rimed dendrites are on average thicker than pristine dendrites, it might be concluded from these comparisons that an aspect ratio of 0.11 might be too large for pristine dendrites, but it could be generally adequate for lightly rimed dendrites. The highest depolarization values at slant viewing for slightly rimed dendrites are about 3 dB lower than for pristine dendrites. The lowest depolarization at the zenith direction is approximately the same. Unlike for the SLDR, reflectivity values depend on particle concentration, so some local increases and decreases in observed Z_{co} (e.g., at around $30^\circ\text{--}40^\circ$ and $120^\circ\text{--}135^\circ$ in the lower frame of

Fig. 8) could be caused by changes in the number of particles.

Some smaller, irregular snowflakes with larger rimed, broad arm stellar and dendritic crystals and other planar-type hydrometeors (e.g., hexagonal plates) were observed at around 2030 UTC 25 January 2011. Note that plates and dendrites exhibit similar depolarization trends with radar elevation angle (Reinking et al. 2002). Broad arm stellar crystals and dendrites have similar aspect ratio and bulk density properties (Pruppacher and Klett 1978). The corresponding SWACR RHI scan ($\text{az} = 87.1^\circ$) and a particle photograph are shown in Figs. 9 and 10 (upper frame), respectively. The observed precipitating cloud during this event was significantly thicker compared to the events in previous examples. Nevertheless, the area where SLDR can be reliably estimated is smaller (Fig. 9c) compared to the area where echoes from the main polarization channel are available (Fig. 9a), because signals in the “weak” (i.e., cross polarization) channel are sometimes not strong enough to get meaningful estimates of depolarization.

The PIP data at the SPL provided estimates of particle mean effective diameters, which were generally between about 1 and 1.5 mm. Typical average wind speeds were about $1\text{--}2 \text{ m s}^{-1}$. Despite the evidence of riming from particle in situ samples, no measurable liquid water was detected by the MWR observations between about 2000 and 2300 UTC. The FSSP-based estimates at the SPL site indicated traces of LWC during the time of the scan in Fig. 9. It can be suggested that rimed particles were advected from different areas.

For the scan in Fig. 9, the constant-altitude SLDR data as a function of the radar elevation angle are shown in Fig. 10 (middle frame). In the lower part of the cloud, the changes in SLDR with elevation angle still clearly exhibit trends that are characteristic of planar crystals (i.e., stellars, dendrites, and hexagonal plates), although the SLDR differences between zenith and slant viewing are significantly smaller compared to pristine and slightly rimed dendrites in Figs. 6 and 8 (middle frames). These differences can be explained by a more spherical shape of predominant hydrometeors (i.e., by increasing value of r as a result of riming) or/and by a decrease of particle effective density. Theoretical estimates of SLDR for two sets of assumptions for aspect ratios and densities of oblate particles are also shown in Fig. 10 (middle frame). These two assumption sets (i.e., $r = 0.5, \rho = 0.55 \text{ g cm}^{-3}$ and $r = 0.25, \rho = 0.35 \text{ g cm}^{-3}$) provide almost identical SLDRs. In the lower part of the echo in Fig. 10 (lower frame), zenith direction enhancements of main channel reflectivity is in somewhat better agreement with the assumption of $r = 0.5, \rho = 0.55 \text{ g cm}^{-3}$, though the Z_{co} difference

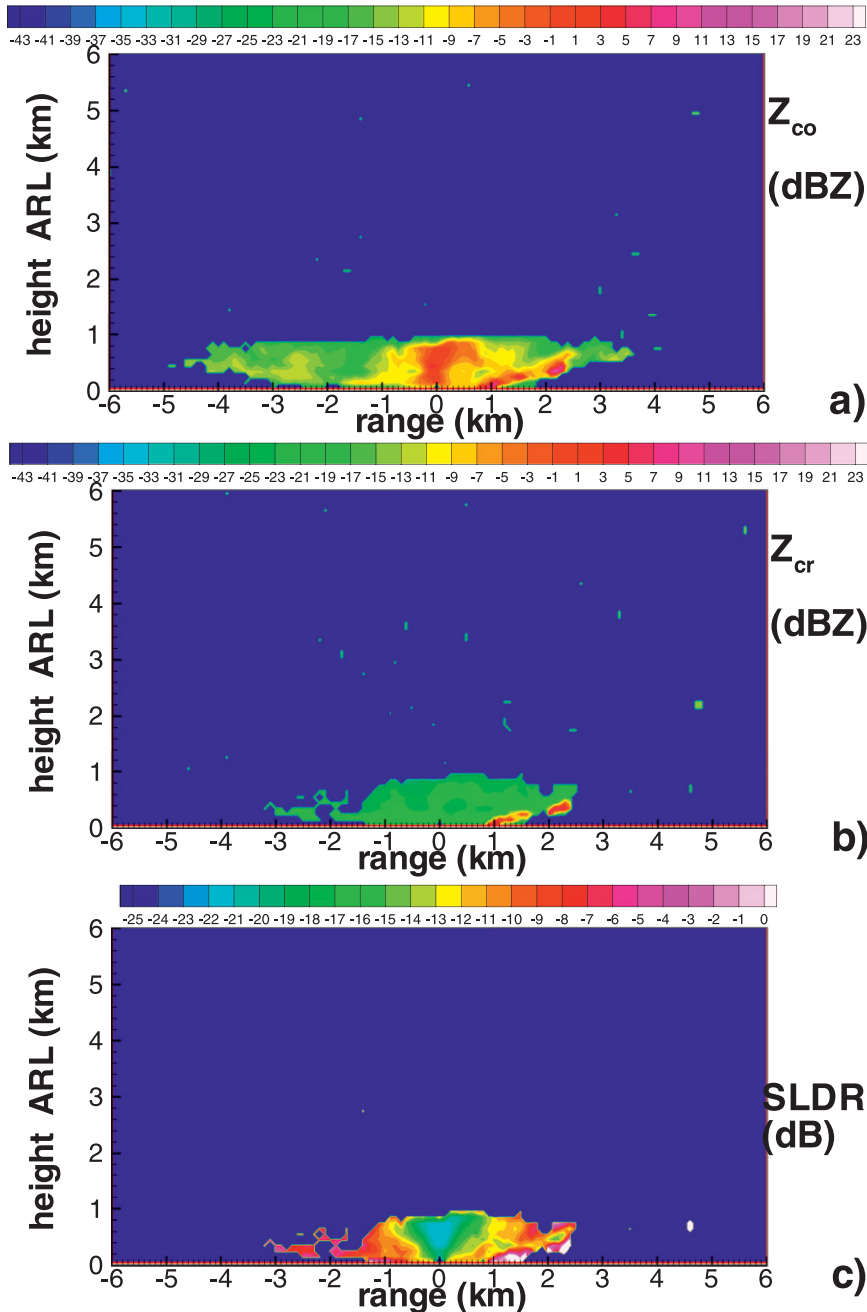


FIG. 7. SWACR measurements of (a) copolar and (b) cross-polar reflectivity and (c) SLDR during the RHI scan toward the SPL ($az = 87.1^\circ$) when observing lightly rimed dendrites at 1823 UTC 26 Jan 2011.

between these two different assumption sets is relatively small.

There are distinctly different SLDR and Z_{co} elevation angle trends in the upper part of the echo (i.e., the data for 1.55 km ARL in Fig. 10, middle and lower frames). Both the SLDR and Z_{co} changes with viewing angle are less distinct at higher altitudes. This suggests a change in the predominant particle type at these altitudes, which

results in differing aspect ratios and/or bulk densities, with apparently more spherical and/or less dense particles at higher altitudes in the cloud.

The presented results illustrate an ambiguity in estimating predominant particle shape from polarimetric radar observations. Ambiguity exists for the observational cases that fall between dry pristine dendrites (showing the maximum SLDR of about -8 dB or so at

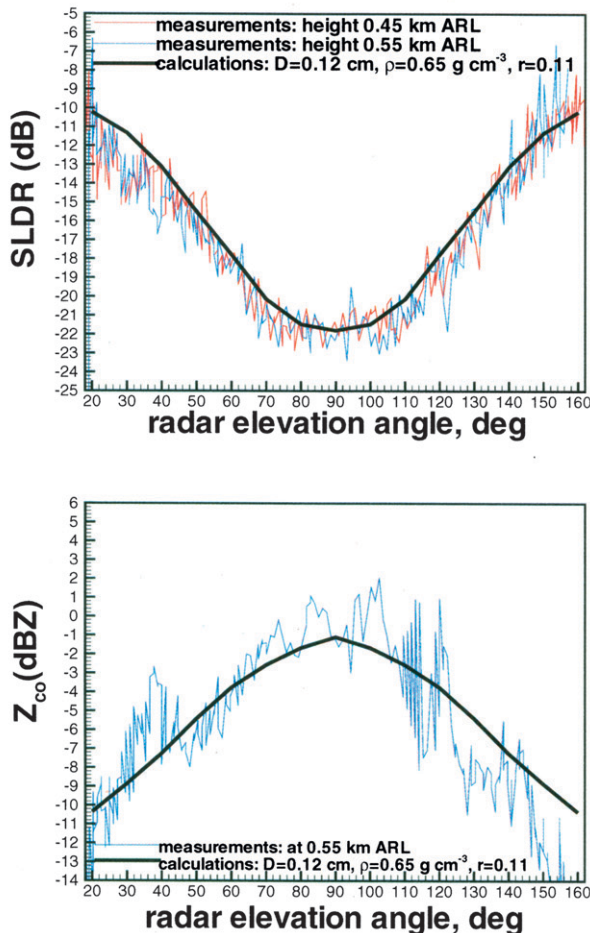


FIG. 8. (top) A particle photograph (small ruler ticks are millimeters), (middle) SLDR, and (bottom) Z_{co} data during the RHI scan shown in Fig. 7.

slant viewing, and values that are close to the cross-coupling limit at zenith viewing) and rounded particles (exhibiting no elevation angle trends in SLDR at values near the SLDR cross-coupling limit). To resolve this ambiguity, a bulk particle density assumption is needed for estimating predominant aspect ratio.

One way of making this assumption is to use the density–size relations developed from microphysical studies. Often such studies provide density (or mass)–size relations where the particle size is expressed in terms of major dimension and a spherical shape is assumed when calculating density from particle mass. In this case, for example, a density value of about 0.09 g cm⁻³ for a spherical particle would correspond to a density of 0.35 g cm⁻³ for an oblate spheroidal particle with an aspect ratio of 0.25 (i.e., one of the assumption used for calculations shown in Fig. 10). Development of a detailed remote sensing technique for estimating the aspect ratios is, however, outside the scope of this study, which is mainly focused on analyzing observational evidence of radar polarization patterns for different hydrometeor types.

4. Observations of dendrite aggregates, mixtures of habits, and columnar crystals

For the cases analyzed in the previous section, larger observed hydrometeors were mostly single crystals (according to surface observers at the SPL) and their measured SLDR values in the zenith direction were typically within about 1 dB or so from the cross-coupling limit. The pattern of increasing SLDR with departure of the viewing direction from zenith (except for rounded graupel or spherical drizzle particles) was observed. This pattern is consistent with the general planar (i.e., oblate) shape of these hydrometeors. At K_a band, aggregates of dendrites also provide the same general planar particle SLDR pattern, although the change in SLDR from zenith to slant viewing is significantly reduced compared to single crystal populations (e.g., Reinking et al. 2002). SWACR observations indicate that this is also the case for W-band data.

Examples of SLDR and main channel reflectivity Z_{co} elevation angle dependences when aggregates of dendrites and some smaller irregulars were the predominant habits are shown in Fig. 11 for two azimuthal directions. This observation was conducted at 2130 UTC 31 January 2011 (the corresponding RHI scan measurements are not shown). Average wind speeds were around 3–4 m s⁻¹ during this event. A particle photograph taken at the SPL is shown in the upper frame of this figure. The changes in SLDR for the 0° RHI are more or less symmetric around the zenith direction, while some small asymmetry is observed for the SLDR pattern in the 87.1° RHI scan at the elevation angles larger than 130°. This might suggest some subtle spatial differences in general aggregate shapes. Main channel reflectivity measurements still show some signal enhancement for near-zenith viewing; Z_{co} elevation angle patterns,

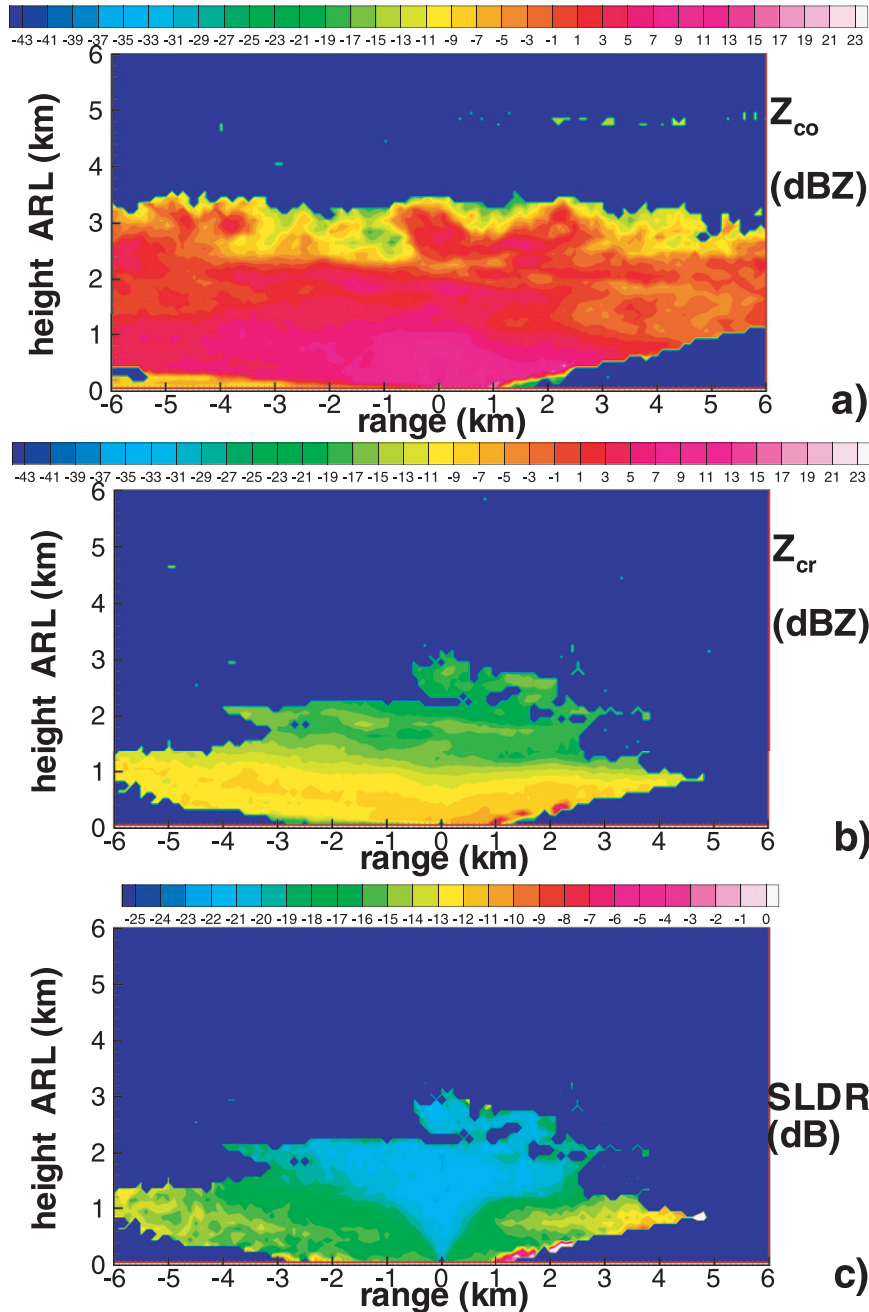


FIG. 9. SWACR measurements of (a) copolar and (b) cross-polar reflectivity and (c) SLDR during the RHI scan toward the SPL ($az = 87.1^\circ$) when observing moderately rimed stellar and dendritic crystals with smaller irregular and hexagonal plates at 2036 UTC 25 Jan 2011.

however, are much less symmetrical than those of SLDR, which is likely due to variability in hydrometer concentrations at different viewing directions.

Given the general SLDR increase as the viewing angle departs from the zenith direction, dendrite aggregates can be considered as planar (oblate) particles. Such particles are, however, more spherical than individual

dendrites. In some way, the SLDR elevation angle dependence for aggregates of dendrites is similar to the pattern of moderately rimed dendrites/stellars (Fig. 10), so distinguishing between these two hydrometeor types could be difficult from polarimetric measurements alone. Because aggregates are generally larger than individual crystals (e.g., the PIP estimates of particle

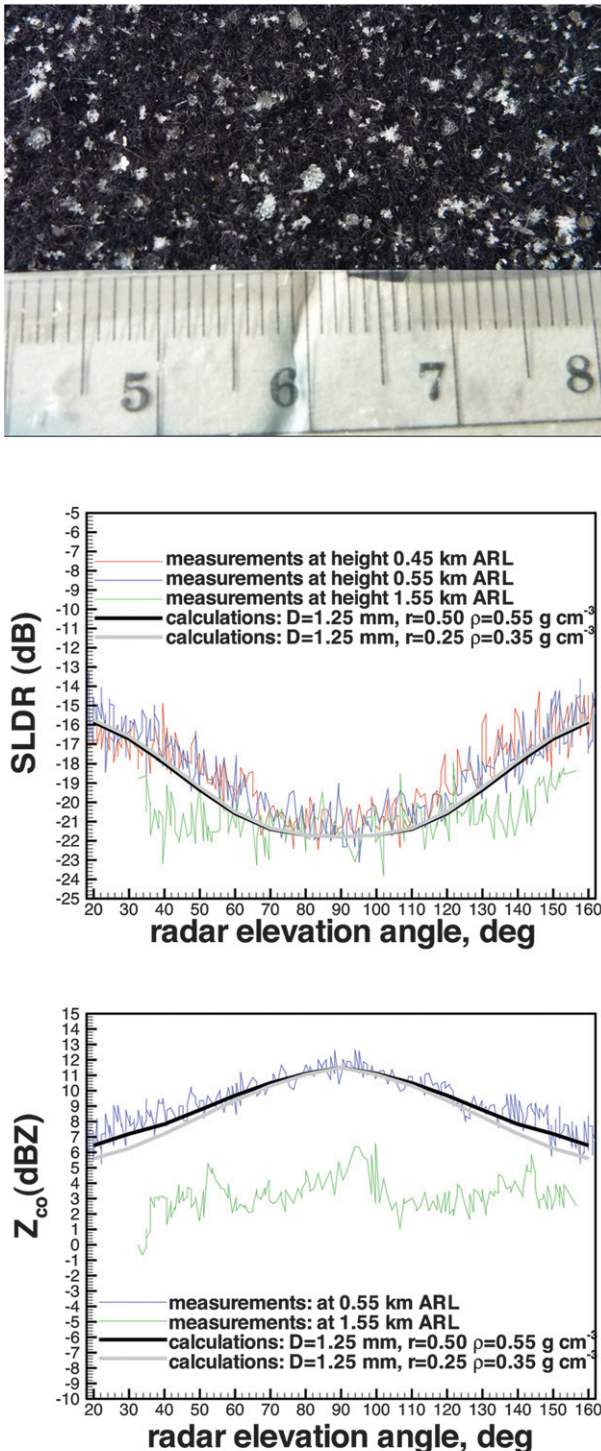


FIG. 10. (top) A particle photograph (small ruler ticks are millimeters) and (middle) constant-altitude SLDR and (bottom) Z_{co} data during the RHI scan shown in Fig. 9.

sizes during these observations indicated the mean effective diameters of about 2 mm, sometimes reaching 4 mm), dual-frequency ratio (DFR) radar estimates of particle sizes can potentially help here because DFR measurements are sensitive to characteristic particle size but exhibit relatively minor variations resulting from bulk density changes (e.g., Matrosov 1993, 2011).

Many SWACR depolarization observations of hydrometeors during StormVEx exhibited SLDR trends indicative of planar (i.e., oblate) or rounded/irregular particle habits. These trends show the SLDR increase from the value near the polarization cross coupling of about -21.8 dB as the viewing angle progressively departs from the zenith direction (for planar-type crystals), or little change in SLDR with elevation angle and values near the cross coupling (for rounded and/or irregular particles). In some instances, however, SLDR values, while still exhibiting a general planar (oblate) particle depolarization pattern as a function of radar elevation angle, were higher than the cross-coupling limit near the zenith direction.

One such instance is shown in Fig. 12, where SLDR and Z_{co} are plotted for the RHI scan from 1750 UTC 31 January 2011. The mean SLDR values in the zenith direction are near -19 dB, which is noticeably higher than the cross-coupling limit. A planar particle depolarization pattern (though not a strong one), however, exists as SLDR values at slant viewing are, on average, 2 dB higher than those in the zenith direction. An examination of particle photos coincident with the radar data (upper panel of Fig. 12) reveals the existence of irregular particles with some rimed dendrites and columnar-type particles. At this time the SPL reported LWC estimates of about 0.1 g m⁻³, as opposed to only traces of LWC reported later in the day for the 2130 UTC scan (Fig. 11), when aggregates of dendrites were mostly observed.

The columnar particles have depolarization patterns (i.e., SLDR elevation angle trends) that are quite different from the planar crystals. For such particles, depolarization ratios generally do not exhibit pronounced changes with elevation angle, and SLDR values can be significantly higher than the cross-coupling limit at all viewing directions. Columnar particles can be modeled as prolate spheroids (e.g., Reinking et al. 2002). Figure 13 shows model calculations of SLDR for prolate spheroids with different assumptions of bulk density and aspect ratio. Similar to the modeling of planar (oblate) habits, it was assumed that particles are oriented on average with their major dimensions in the horizontal plane, with a standard deviation of 9° representing particle flutter. The azimuthal orientation of particle major

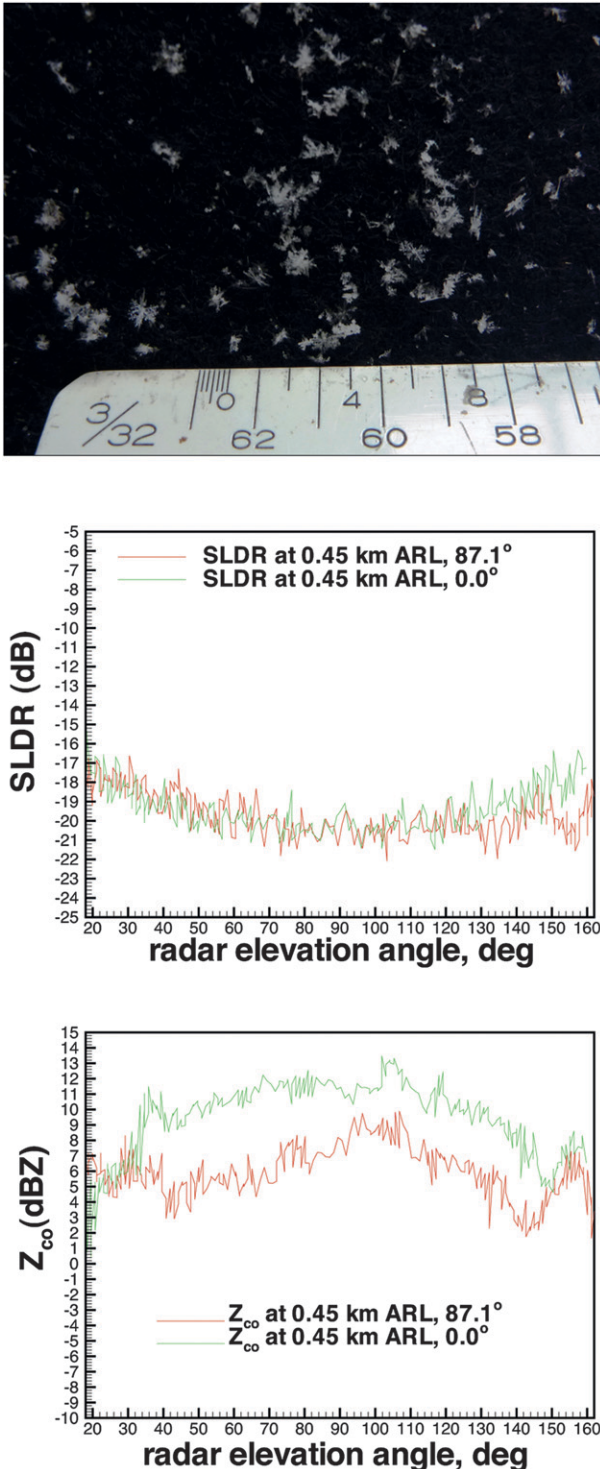


FIG. 11. (top) A particle photograph (the big ticks on the ruler are 0.47 cm apart), (middle) SLDR, and (bottom) Z_{co} elevation angle dependences for RHI scans at 2130 UTC 31 Jan 2011 when aggregates of dendrites were the predominant particle type.

axes was assumed random. Results do not exhibit significant sensitivity to the choice of the orientation standard deviation if it is less than about 10° – 15° .

As seen from the modeling results (Fig. 13), there are no significant trends in SLDR with radar elevation angle, except for limited changes (generally within few decibels) for some angles. These limited changes are due to non-Rayleigh scattering effects at W band because they are not usually present for modeling results at lower radar frequencies (e.g., Matrosov et al. 2001). The offset of the mean SLDR from the radar cross-coupling value depends primarily on aspect ratio and bulk density assumptions, and different combinations of r and ρ can produce similar offsets. Compared to planar hydrometeors, columnar particles produce significantly higher depolarization at vertical viewing due to the fact that SLDR reaches its maximum when particles are in the incident wave polarization plane and their long axes are oriented at 45° relative to the transmitted polarization direction. Particles with such orientations are present for both vertical and slant viewing. In the event of planar hydrometeors, the minimum depolarization is observed at vertical viewing because their aspect ratio projections are close to the unity for this observation geometry. Unlike SLDR, measurements of differential reflectivity Z_{DR} , which is usually available with precipitation polarimetric radars, generally cannot be used to distinguish between planar and columnar habits.

It is likely that a small amount of columnar-type hydrometeors contributed to the total depolarization for the case in Fig. 12, while the general elevation angle pattern was still influenced by planar (oblate)-type particles. Some influence of columnar crystals is also not out of question for the scan in Fig. 11, because occasional columnar (prolate)-type particles can also be seen in the photograph for this case. For that scan, however, the zenith direction SLDR increase over the cross-coupling value of about -21.8 dB was only approximately 1 dB.

The StormVEx dataset also includes observational events when columnar particles were the dominant hydrometeor habit, though these events were not as numerous as those with planar crystals as a dominant habit. One such event was recorded on 4 March 2011 when a cloud with relatively low reflectivity near the ground (< -7 dBZ) was observed. The StormVEx scientists at the SPL reported that cloud imaging probes indicated mostly columnar crystals during this observation period (no photographs were taken at this time). An example of the SWACR SPL RHI scan for this event is shown in Fig. 14. There was no measurable precipitation at the ground at the observation time. The copolar reflectivity (Fig. 14a) is rather small and there are no near-zenith direction enhancements. SLDR values (Fig. 14c) do not

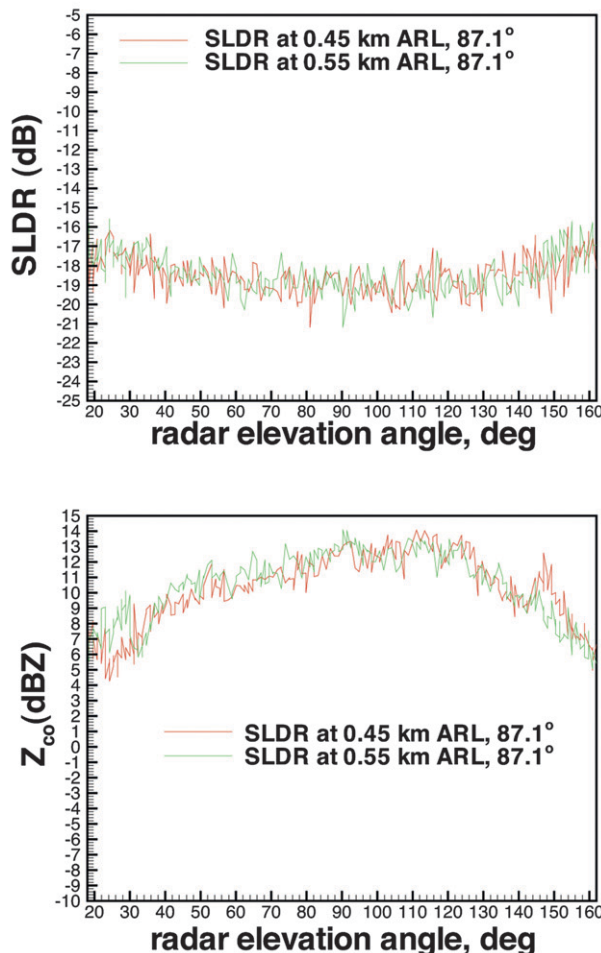
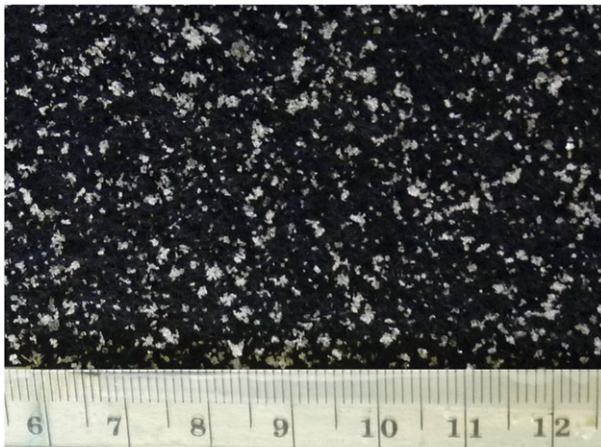


FIG. 12. (top) A particle photograph (small ruler ticks are millimeters) and (middle) SLDR, and (bottom) Z_{co} elevation angle dependences for RHI scans at 1750 UTC 31 Jan 2011 when some columnar particles were present in the hydrometeor mixture.

show any trends associated with changes in the radar elevation angle. There are also no obvious changes in SLDR for certain viewing directions, which could exist, in part, due to non-Rayleigh scattering effects. These effects are likely to be averaged out as some variability of hydrometeor habits and characteristic sizes in the radar resolution volume can be expected.

The elevation angle dependences of constant altitude SLDR and Z_{co} corresponding to the scan shown in Fig. 14 are depicted in Fig. 15. As expected from the theoretical modeling presented in Fig. 13, there are no significant trends in SLDR depending on the direction of observations. The mean SLDR value is about -18 dB, which is noticeably higher than the estimated cross-coupling limit. As mentioned previously, different combinations of particle aspect ratios and bulk densities can result in similar SLDR offsets, so a bulk density assumption would be important when trying to estimate the effective aspect ratio from depolarization measurements. As for SLDR, no clear trends are present in main channel reflectivity measurements as a function of elevation angle. The Z_{co} variability, however, is stronger compared to SLDR, which is likely due to changes in particle concentrations at different viewing directions. SLDR patterns for RHI scans in other direction were similar (not shown).

5. Discussion and conclusions

Some earlier studies (e.g., Matrosov et al. 2001; Reinking et al. 2002; Aydin and Singh 2004) indicated the possibility of millimeter-wavelength cloud radar polarimetric measurements to identify ice hydrometeor types. This study provides further evidence that depolarization measurements can be used for identification of dominant ice particle habits and estimation of their shapes, and thus for future studies of ice hydrometeor microphysics and prevalent particle growth processes (e.g., vapor deposition versus aggregation). The slant 45° linear polarization for the ARM SWACR radar was chosen for ice hydrometeor studies because SLDR measured at this polarization state is less susceptible to particle orientation than LDR measured when traditional horizontal-vertical polarization states are used. Although CDR is even less sensitive to particle orientation than SLDR at slant viewing (e.g., Matrosov et al. 2001), it was not used because of difficulties in implementing circular polarization measurements with the SWACR.

Observations were performed for a variety of ice hydrometeor types ranging from quasi-spherical graupel, which provided a very small mean depolarization ratio offset (~ 0.4 dB) with respect to the estimated radar cross-coupling limit of about -21.8 dB, to pristine dry dendrites, which exhibited the highest SLDR values

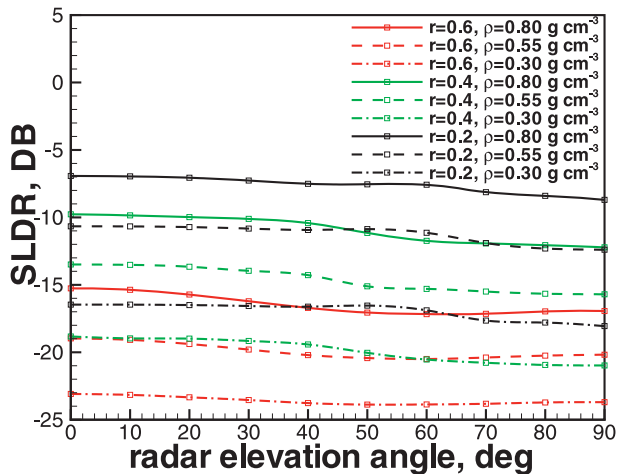


FIG. 13. Model calculations of SLDR vs radar elevation angle for columnar (prolate)-type particles for different aspect ratio and density assumptions, $D = 1$ mm.

of about -8 dB at slant elevation directions, to columnar crystals with elevated SLDR values that did not significantly change with viewing direction. Many experimental events containing a mixture of observed habits (e.g., rimed dendrites, aggregates, irregulars, nonrounded graupel, and planar-columnar habit mixtures) exhibited elevation angle patterns somewhere between those observed for the extreme cases of spherical particles and dry pristine dendrites. Distinct depolarization dependence on the viewing angle indicates a high degree of ice hydrometeor orientation.

Relatively simple model calculations using the T-matrix approach for spheroidal particles with appropriate assumptions, which approximate overall particle aspect ratio and bulk density, satisfactorily explained the SWACR-observed depolarization ratios and their dependence on radar elevation angle. While changes in SLDR with the SWACR elevation angle are different in magnitude from those for lower-frequency radars, this particle model also performed well for K_a -band depolarization data (Matrosov et al. 2001; Reinking et al. 2002). Combined effects of non-Rayleigh scattering, particle nonsphericity, density, and orientation result in higher values of absolute radar reflectivities near the zenith direction compared to the slant viewing angles. These effects are more pronounced for planar-type particles with a higher degree of nonsphericity and larger density, and are relatively small for aggregates, irregular particles, and columnar hydrometeors. The T-matrix theoretical calculations explained the tendencies for the observed reflectivity increase, though the magnitude of the enhancement is subject to a greater variability (compared to SLDR) resulting from changes in particle size. The reflectivity enhancement effect

is stronger at W band compared to lower radar frequencies. While T-matrix method calculations for the spheroidal shape model were able to roughly match observed single-frequency SLDR measurements, studies with the use of more complex particle shapes and/or computational approaches will be needed in the future to better understand limitations of this model. One drawback of the T-matrix method is its general inability to model particles with very low aspect ratios, which might be necessary to better describe scattering by some pristine crystals.

Many of the hydrometeors observed during Storm VEx exhibited planar crystal type habits, with the smallest SLDR values in the zenith direction (near the polarization cross-coupling value) and an SLDR increasing trend as the viewing angle moves away from zenith. The rate of increase is most pronounced at viewing angles of about 40° – 50° . Some prolate-type hydrometeors (e.g., columns) in the particle population can increase the total depolarization near the zenith direction, although if planar (oblate)-type particles are still the predominant habit, then a general SLDR increase retains as viewing moves off zenith.

Cases when columnar particle types were the predominant habit were also observed. For these cases, SLDR values generally did not exhibit significant trends with changing viewing angle and significant depolarization offsets from the cross-coupling value were present for all viewing directions (including zenith viewing). Theoretical modeling indicates that such relatively neutral SLDR elevation angle patterns are expected for columnar crystals that are randomly oriented in azimuth, with their major dimensions being approximately in the horizontal plane. In the absence of strong electrical fields, this type of orientation is dictated by aerodynamic forcing.

Overall, the elevation angle dependence of SLDR can be used to differentiate between predominant hydrometeor habits (i.e., planar hydrometeors, such as dendrites and stellars with variable degree of riming, plates, and aggregates of dendrites versus columnar hydrometeors). Note that the elevation angle patterns of other common polarimetric radar measurable, such as differential reflectivity (Z_{DR}), do not readily provide differentiation between columnar and planar hydrometeor habits (e.g., Matrosov 2004). For the planar crystal type, the magnitude of change in SLDR values between the zenith and the lowest viewing angles or the average depolarization value at the mean slant (e.g., at about 45° radar elevation viewing) are indicative of the aspect ratio of the predominant particles. The mean slant depolarization values could be less susceptible to differences in the particle orientation flutter compared to the difference in depolarization ratios between the zenith and lowest viewing angles (e.g., Matrosov et al. 2001).

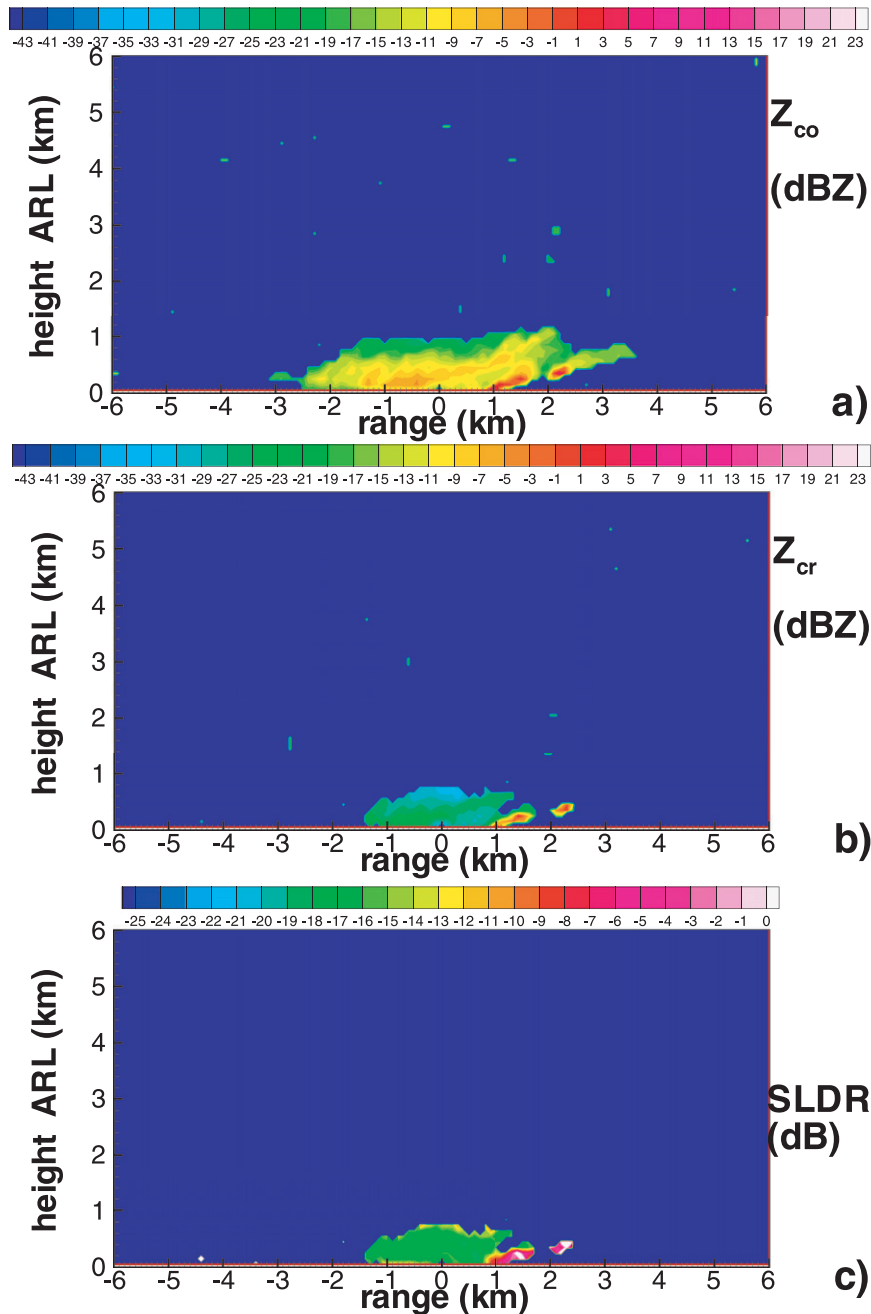


FIG. 14. SWACR measurements of (a) copolar and (b) cross-polar reflectivity and (c) SLDR during the RHI scan toward the SPL ($az = 87.1^\circ$) when observing predominantly columnar crystals at 0341 UTC 4 Mar 2011.

The particle bulk density also influences the depolarization angular dependence such that different combinations of mean aspect ratio and density can explain the observed SLDR. For columnar particles, the mean SLDR offset from the polarization cross-coupling value is indicative of the hydrometeor aspect ratio, although this offset also depends on particle density.

Future remote sensing techniques for estimating ice hydrometeor habits should aim to decouple between the density and shape effects. This might be achieved, for example, by independently estimating particle characteristic size [e.g., from dual-frequency or Doppler radar approaches, or, in simpler case, from correlations between characteristic size and reflectivity (e.g., Matrosov

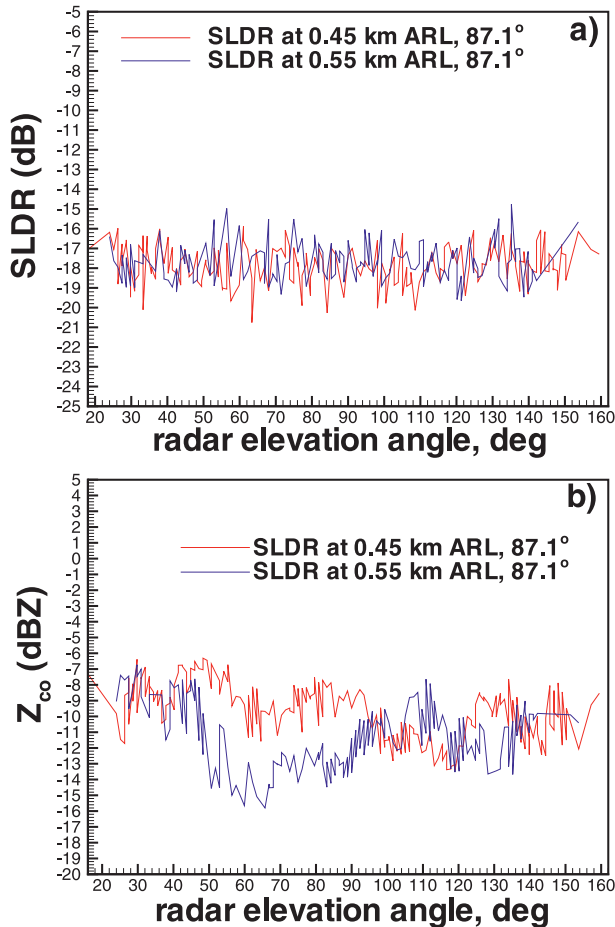


FIG. 15. (a) SLDR and (b) Z_{co} elevation angle dependences for the RHI scan toward the SPL at 0341 UTC 4 Mar 2011 when columnar particles were the predominant habit.

1997)], which can subsequently be used to constrain the particle density assumption. Particle characteristic size, to a certain degree, also influences the dynamic range of depolarization changes. Development of such remote sensing techniques, however, is beyond the scope of this study, which is focused on providing observational evidence that W-band radar polarimetric measurements contain information on ice hydrometeor habits. Because of the nature of radar measurements, ice particle habit information inferred from polarimetric observations represents the dominant shape of particles that provide the largest contribution to radar signals. In other words, it is the reflectivity-weighted information. This is, however, the characteristic feature of all radar-based remote sensing retrievals.

The SWACR depolarization ratios were primarily available at relatively closer ranges (within a few kilometers) because at longer ranges the cross-polar reflectivities were typically weaker than copolar reflectivities

by one to two orders of magnitude. This limitation precluded SLDR estimations in higher-altitude ice clouds. To reliably observe such clouds in the cross-polar channel, the radar sensitivity needs to be increased. Another approach to enhance depolarization ratios is to perform measurements using some special elliptical polarizations, which can provide a signal increase in the “weak” radar channel, although at the expense of the dynamic range of depolarization ratio changes.

Acknowledgments. The StormVEx campaign and all measurements included in this study were supported by the Office of Biological and Environmental Research of the U.S. Department of Energy as part of the Atmospheric Radiation Measurement Climate Research Facility. This campaign was a success because of extraordinary support from the AMF2 staff and managers, the SPL permanent and local volunteer staff, the Steamboat Ski and Resort Corporation, the U.S. Forest Service, the Grand Junction National Weather Service Office, the ARM radar engineers (Kevin Widener and Nitin Bharadwaj), and a team of graduates students (Betsy Berry, Stewart Evans, Ben Hillman, Will Mace, Clint Schmidt, Carolyn Stwertka, Adam Varble, and Christy Wall).

REFERENCES

- Avramov, A., and J. Y. Harrington, 2010: The influence of parameterized ice habit on simulated mixed phase Arctic cloud. *J. Geophys. Res.*, **115**, D03205, doi:10.1029/2009JD012108.
- Aydin, K., and C. Tang, 1997: Relationships between IWC and polarimetric radar measurands at 94 and 220 GHz for hexagonal columns and plates. *J. Atmos. Oceanic Technol.*, **14**, 1055–1063.
- , and J. Singh, 2004: Cloud ice crystal classification using a 95-GHz polarimetric radar. *J. Atmos. Oceanic Technol.*, **21**, 1679–1688.
- Barber, P., and C. Yeh, 1975: Scattering of electromagnetic waves by arbitrarily shaped dielectric bodies. *Appl. Opt.*, **14**, 2864–2872.
- Botta, G., K. Aydin, J. Verlinde, A. E. Avramov, A. S. Ackerman, A. M. Fridlind, G. M. McFarquhar, and M. Wolde, 2011: Millimeter wave scattering from ice crystals and their aggregates: Comparing cloud model simulations with X- and Ka-band radar measurements. *J. Geophys. Res.*, **116**, D00T04, doi:10.1029/2011JD015909.
- Brunkow, D., V. N. Bringi, P. C. Kennedy, S. A. Rutledge, V. Chandrasekar, E. A. Mueller, and R. K. Bowie, 2000: A description of the CSU–CHILL national radar facility. *J. Atmos. Oceanic Technol.*, **17**, 1596–1608.
- Galletti, M., D. S. Zrnic, V. M. Melnikov, and R. J. Doviak, 2012: Degree of polarization at horizontal transmit: Theory and applications for weather radar. *IEEE Trans. Geosci. Remote Sens.*, **9**, 383–387.
- Greco, M., and W. S. Olson, 2008: Precipitating snow retrievals from combined airborne cloud radar and millimeter-wave

- radiometer observations. *J. Appl. Meteor. Climatol.*, **47**, 1634–1650.
- Hogan, R. J., L. Tian, P. R. A. Brown, C. D. Westbrook, A. J. Heymsfield, and J. D. Eastment, 2012: Radar scattering from ice aggregates using the horizontally aligned oblate spheroid approximation. *J. Appl. Meteor. Climatol.*, **51**, 655–671.
- Ishimoto, H., 2008: Radar backscattering computations for fractal-shaped snowflakes. *J. Meteor. Soc. Japan*, **86**, 459–469.
- Kneifel, S., M. S. Kulie, and R. Bennartz, 2011: A triple-frequency approach to retrieve microphysical snowfall parameters. *J. Geophys. Res.*, **116**, D11203, doi:10.1029/2010JD015430.
- Kollias, P., E. E. Clothiaux, M. A. Miller, E. P. Luke, K. L. Johnson, K. P. Moran, K. W. Widener, and B. A. Albrecht, 2007: The atmospheric radiation measurement program cloud profiling radars: Second-generation sampling strategies, processing, and cloud data products. *J. Atmos. Oceanic Technol.*, **24**, 1199–1214.
- Liu, G., 2008: A database of microwave single scattering properties for nonspherical ice particles. *Bull. Amer. Meteor. Soc.*, **89**, 1563–1570.
- Matrosov, S. Y., 1991: Theoretical study of radar polarization parameters obtained from cirrus clouds. *J. Atmos. Sci.*, **48**, 1062–1070.
- , 1993: Possibilities of cirrus particle sizing from dual-frequency radar measurements. *J. Geophys. Res.*, **98** (D11), 20 675–20 683.
- , 1997: Variability of microphysical parameters in high-altitude ice clouds: Results of the remote sensing method. *J. Appl. Meteor.*, **36**, 633–648.
- , 2004: Depolarization estimates from linear H and V measurements with radar radars operating in simultaneous transmission-simultaneous receiving mode. *J. Atmos. Oceanic Technol.*, **21**, 574–583.
- , 2007: Modeling backscatter properties of snowfall at millimeter wavelengths. *J. Atmos. Sci.*, **64**, 1727–1736.
- , 2011: Feasibility of using radar differential Doppler velocity and dual-frequency ratio for sizing particles in thick ice clouds. *J. Geophys. Res.*, **116**, D17202, doi:10.1029/2011JD015857.
- , R. F. Reinking, R. A. Kropfli, and B. W. Bartram, 1996: Estimation of ice hydrometeor types and shapes from radar polarization measurements. *J. Atmos. Oceanic Technol.*, **13**, 85–96.
- , —, —, B. E. Martner, and B. W. Bartram, 2001: On the use of radar depolarization ratios for estimating shapes of ice hydrometeors in winter clouds. *J. Appl. Meteor.*, **40**, 479–490.
- , A. J. Heymsfield, and Z. Wang, 2005a: Dual-frequency ratio of nonspherical atmospheric hydrometeors. *Geophys. Res. Lett.*, **32**, L13816, doi:10.1029/2005GL023210.
- , R. F. Reinking, and I. V. Djalalova, 2005b: Inferring fall attitudes of pristine dendritic crystals from polarimetric radar data. *J. Atmos. Sci.*, **62**, 241–250.
- Okamoto, H., 2002: Information content of the 95-GHz cloud radar signals: Theoretical assessment of effects of nonsphericity and error evaluation of the discrete dipole approximation. *J. Geophys. Res.*, **107**, 4628, doi:10.1029/2001JD001386.
- Petty, G. W., and W. Huang, 2010: Microwave backscatter and extinction by soft ice spheres and complex snow aggregates. *J. Atmos. Sci.*, **67**, 769–787.
- Pruppacher, H. R., and J. D. Klett, 1978: *Microphysics of Clouds and Precipitation*. D. Reidel, 714 pp.
- Reinking, R. F., S. Y. Matrosov, R. T. Bruintjes, and B. E. Martner, 1997: Identification of hydrometeors with elliptical and linear polarization K_a-band radar. *J. Appl. Meteor.*, **36**, 322–339.
- , —, R. A. Kropfli, and B. W. Bartram, 2002: Evaluation of a slant 45° slant quasi-linear radar polarization for distinguishing drizzle droplets, pristine ice crystals, and less regular ice particles. *J. Atmos. Oceanic Technol.*, **19**, 296–321.
- Ryzhkov, A. V., T. J. Schuur, D. W. Burgess, P. L. Heinselman, S. E. Giangrande, and D. S. Zrnic, 2005: The Joint Polarization Experiment. *Bull. Amer. Meteor. Soc.*, **86**, 809–824.
- Schneider, T. L., and G. L. Stephens, 1995: Theoretical aspects of modeling backscattering by ice particles at millimeter wavelengths. *J. Atmos. Sci.*, **52**, 4367–4385.
- Westbrook, C. D., R. C. Ball, and P. R. Field, 2006: Radar scattering by aggregate snowflakes. *Quart. J. Roy. Meteor. Soc.*, **132**, 897–914, doi:10.1256/qj.05.82.